Rev. Adv. Mater. Sci. 54 (2018) 1-13

ON THE COMMON ORIGIN OF STRUCTURAL SUPERPLASTICITY IN DIFFERENT CLASSES OF MATERIALS

K.A. Padmanabhan[1] and M. Raviathul Basariya[2]

[1]Research and Innovation Advisory Board, Tata Consultancy Services (TCS) & Research Advisor, TCS & Aditya Birla S&T Company, IIT-Madras Research Park, Taramani, Chennai 600013, India
[2]Independent Researcher; formerly of IIT-BHU, Varanasi and Anna University, Chennai, India

Received: April 23, 2018

Abstract. The present model starts with an assumption that grain/ interphase boundary sliding (GBS) that is dominant during optimal superplastic flow is slower than the accommodation processes of dislocation emission from sliding boundaries, highly localized diffusion in the boundary regions and/ or grain rotation that are present as a concomitant of the GBS process. When boundary sliding develops to a mesoscopic scale (of the order of a grain diameter or more), by the alignment of contiguous boundaries, plane interface formation/ mesoscopic boundary sliding is observed. Significant and simultaneous sliding along different plane interfaces and their interconnection can lead to large scale deformation and superplasticity. The accommodation steps, being faster than GBS, do not enter the strain rate equation. Mathematical development of these ideas using transition state theory results in a transcendental strain rate equation for steady state optimal superplastic flow, which when solved numerically helps one to describe the phenomenon quantitatively in terms of two constants, the activation energy for the rate controlling process, ΔF_0 and the threshold stress needed to be overcome for the commencement of mesoscopic boundary sliding, σ_0.The analysis also explains quantitatively texture randomization as a function of superplastic strain.
It is also pointed out, without going into details, that recently the problem has been reduced to FOUR "universal" constants, viz. the mean strain associated with a unit boundary sliding event γ_0, specific grain boundary energy γ_B, which is assumed to be isotropic, *N* the average number of boundaries that align to form a plane interface during mesoscopic boundary sliding and "*a*" a grain-size- and shape- dependent constant that obeys the condition $0 < a < 0.5$, in terms of which one can account for superplasticity in any material. In combination with the regression equations popularized by Frost and Ashby to predict the shear modulus of any material at any temperature, these four constants allow one to predict the steady state strain rate of any structurally superplastic material accurately, including those whose superplastic response is not considered for the analysis. The details of the last mentioned result, which are unpublished, will be presented elsewhere.

1. INTRODUCTION

OUR BELIEF: The present authors believe that "to the same natural effects we must, as far as possible, assign the same causes" (Hawking, S., 2003. On the Shoulders of Giants. Running Press, London, 731). Such an approach would reduce the number of assumptions needed to explain a phenomenon in a unified manner.

Superplasticity, the phenomenon during the occurrence of which polycrystalline materials exhibit near-isotropic, extreme tensile elongations prior to failure, was first reported in the early years of the 20th century. This topic has been reviewed extensively. Of the two categories of superplasticity, namely, environmental superplasticity and structural superplasticity, the latter, which is the concern of the present work is considered to be the behavior

Corresponding author: K.A. Padmanabhan, e-mail: ananthaster@gmail.com; kap@annauniv.edu

exhibited at low strain-rates and deformation temperatures, often greater than half the melting temperature on an absolute scale (sometimes lower), by materials having grain sizes in the micrometer-, sub-micrometer- or nanometer range [1-3]. Environmental superplasticity, superplasticity in large grained materials and the initial, transient stress-strain region in conventional structural superplasticity itself are not examined here.

In general, high temperature deformation is described by an equation analogous to

$$\dot{\varepsilon} = A\left(\frac{\sigma^n}{d^a}\right)\exp\left(-\frac{Q}{kT}\right), \qquad (1)$$

where $\dot{\varepsilon}$ is the strain rate, A and a are material constants, σ is the external stress, n is the stress exponent, d is the average grain size, Q is the activation energy for the rate controlling process, k and T are the Boltzmann constant and absolute temperature of deformation respectively [1-4].The dominance of grain boundary sliding during superplastic flow is known since the days of Pearson [5]. Notwithstanding this, many theories that treat dislocation motion, diffusion or multi-mechanisms as rate controlling have been proposed to explain structural superplasticity [1-3,6,7]. Padmanabhan and Davies [1] consider superplastic deformation as a process in which deforming, interconnected grain/interphase boundaries surround essentially non –deforming grains except for what is required to ensure coherent strain. Over the years their ideas have been developed into a mathematical model [8-12], which proposes a single rate controlling mechanism for superplastic deformation, viz. GBS that develops to a mesoscopic scale. It has been demonstrated to be relevant for understanding optimal superplastic flow in metals and alloys, metal-matrix composites, ceramics, ceramic-matrix composites, intermetallic compounds, dispersion strengthened alloys, metals with a quasi-crystalline phase, nanostructured materials, amorphous materials like bulk metallic glasses, geological materials and polycrystalline ice [13-17]. In the case of minerals, rocks and ice, however, it is more appropriate to state that what has been observed is grain-size-sensitive (GSS) creep, because extreme isotropic elongations in tension are yet to be reported in these classes of materials. However, it does appear that the underlying physical mechanisms in case of rocks and ice also are similar to what are seen in other classes of superplastic materials. The present model, which applies to optimal structural superplastic flow in all classes of materials, is also useful in explaining the transition in material behavior from hardening to softening with decreasing grain size, the so called "inverse Hall-Petch" (IHP) or grain size softening [18-20] effect. Therefore, it does appear that a case can be made that superplasticity is a near-ubiquitous phenomenon, with an underlying common physical cause. For such a statement to be true, the phenomenology of superplastic flow should be similar for different classes of materials. The aim of the present work is to highlight the unified physics of the phenomenon. In addition, some aspects of the model which have not so far been emphasized will be brought into relief. The validation of the model is done by analyzing experimental data pertaining to different classes of superplastic materials. To start with, for completeness, a brief description of the grain/ interphase boundary sliding controlled flow process is presented here, as this model has already been discussed extensively elsewhere [8-23].

2. A MECHANISM FOR MESOSCOPIC GRAIN BOUNDARY SLIDING

Grain boundary sliding (GBS) is considered by most as a dominant physical process present during optimal superplastic flow. Therefore, models proposed for superplasticity involve different accommodation processes, along with GBS. Hazzledine's [24] assertion at an early stage that GBS is an inherently fast process than any of the accommodation processes and that the latter processes only can control the overall rate of deformation has been accepted by many persons working in this field. For GBS to proceed to any significant extent at least one accommodation process is essential and the slowest step will control the rate of flow. Then the correlation of strain rate with stress, grain size and temperature (kinetics of flow) will be determined by the details of the accommodation process assumed. In these cases, in spite of the significant differences in the concepts associated with individual models, the rate equation derived has essentially the same form [25], viz., that of the so called "Dorn equation" (although certain restrictions imposed in the original analysis of Dorn [26] have been relaxed by later workers (for a summary see [27])), which is represented as,

$$\dot{\varepsilon} = \left(AGb/kT\right)\left(b/d\right)^p \times \left(\sigma/G\right)^n \exp\left(-Q/RT\right). \qquad (2)$$

Commenting on these models, Kaibyshev [2] has concluded that in these physics-based models that

end up in Eq. (2), the values of p, n, A, and Q are almost the same, in spite of the varying and at least in some instances conflicting concepts that underlie the models. This, in his opinion, is due to the "numerous assumptions" and "conflicting simplifications" of the physical problem. These models reveal an inability for prediction and can at best rationalize the experimental results under pre-defined conditions in certain materials systems with the help of a few ill-defined, fitting constants, e.g. the value of the relevant diffusivity of the concerned alloy.

In another category fall the analyses like those of [7,28; see Fig. 4 of 28] and [29], which use the "Dorn equation" and also make assumptions about the structure of general/ high-angle grain boundaries which, in our opinion, are not consistent with contemporary views[1]. Gleiter's now well established views and experiments on the structure of general/ high-angle grain boundaries are as follows: (i) there are no coincidence site lattices (CSL's) in general/ high-angle boundaries, and (ii) there are only "structural units" and CSL's in many general boundaries turn out to be not the minimum energy configurations. Gleiter has also pointed out that "solitons", e.g. vacancies, dislocations etc., are not stable in high-angle grain boundaries and they get delocalized once they enter such grain boundaries. (For a summary of these views, see, [11,30] and the few scholarly papers of Sutton and Vitek, who using massive MD simulations, have shown clearly that no CSL's exist in relaxed high-angle grain boundaries [31-36].) Representations like what is shown in Fig. 4 of [28], where the glide of grain boundary dislocations along a boundary triggers a similar process (due to a stress build up at the triple junction, for example,) in an adjacent grain is possible only when coincidence site lattices can be constructed in such boundaries and a description of this kind militates against the now well founded and experimentally verified works of Gleiter, Sutton, Vitek and others [30-36] on the structure of general/ high-angle grain boundaries. It is also pertinent that stress build up at the triple point and its subsequent release during the emission of dislocations into a neighboring grain, as envisaged above, should give rise to an oscillating stress-strain curve during steady state superplastic deformation and such curves have not been observed. Finally, experiments reveal that during steady state, optimal superplastic flow grain rotation that leads to randomization of pre-existing texture is present [1-3]. Diffusion control does not alter the texture, while dislocation control, as suggested in [7,28,29] can only lead to certain preferred orientations dependent on the crystallographic nature of the deformation of the starting material. Therefore, there will be no further discussion on these models/ approaches. Instead, an alternative interpretation of optimal superplastic deformation rate controlled by grain boundary sliding that develops to a mesoscopic scale will be presented. While doing this, it will be ensured (a) that no adjustable constants/ parameters are allowed, and (b) that the analysis applies to all systems that exhibit optimal structural superplasticity.

In the present model [8-15, 23-25], a network of sliding high-angle grain boundaries that are favorably oriented to the stress axis contribute very significantly to superplastic flow. The analysis is carried out at two levels: (a) atomistic, and (b) mesoscopic.

Atomistic level deformation of GBS: Every general/ high-angle boundary is divided into a number of atomic scale ensembles that surround free volume sites present at specific locations on the boundary that depend on its misoreintation. The boundary misorientation and the interatomic forces between the atoms that constitute the boundary determine the free volume fraction present in the boundary. Every such free volume site constitutes a basic unit of sliding. Presence of free volume in such sites makes the shear resistance of these basic sliding units less than that of the rest of the boundary, which consists of (free volume absent) structural units, and so boundary sliding starts at (these free volume) sites simultaneously. For a mathematical development of the ideas, following Eshelby [37] the basic sliding unit is considered to be of an oblate spheroid shape. Any deviation from this shape in a real situation is taken care of by a form factor of near-unit-value [8]. The basic sliding unit is located symmetrically about the plane of the boundary. On an average, the diameter of the oblate spheroid is taken as equal to 5 atomic diameters and its height at the centre, in a direction perpendicular to that of the equatorial diameter, as 2.5 atomic diameters, i.e. a value equal to that of average grain boundary width [38]. An oblate spheroid shape is chosen because

[1]High-angle/ general grain boundaries are the most important structural elements responsible for superplasticity. In the limit, if the entire material has no high-angle/ general grain boundaries, superplasticity is absent, but the same material is superplastic when a significant fraction of the boundaries is of the high-angle type. For a summary of the experimental results in this regard, see [15].

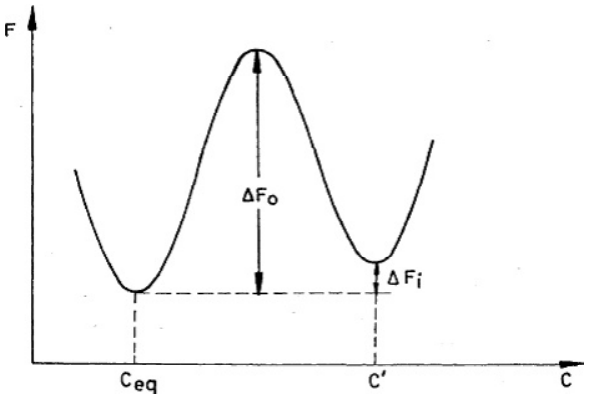

Fig. 1. Relationship between free energy, *F* and atomic configuration, *C* for unit of boundary sliding (see our work [8]).

Eshelby [37] has already shown that the stress-strain field inside a deformed oblate spheroid is uniform and that from the results some important engineering properties of materials can be deduced. In addition, the dimensions of the oblate spheroid have been so chosen as to make the present analysis consistent with that of Argon [39] for the deformation of metallic glasses. A unit boundary sliding event is considered to arise as follows [8-10].

(a) In the entire bulk of the sample, due to the action of a small external stress the atomic ensembles around the free volume sites in the boundary, that constitute the basic sliding units, simultaneously undergo shear transformations and these (sliding) events are essentially independent of one another.

(b) In the absence of an external stress, the atomic arrangement in the basic sliding unit represents the equilibrium or metastable equilibrium configuration, C_{eq} (Fig. 1). This corresponds to the lowest free energy configuration for the given state of the boundary (Fig. 1). It is assumed that as a result of excess free volume in the basic unit there are atomic arrangements slightly different from *C* which correspond to other new low energy metastable configuration *C*'. Thus the total free energy, *F*(*C*') of these states will be $(C)+\Delta F_i$. This additional energy ΔF_i will be provided by the external stress *during a thermal event* to ensure than *C* = *C*'. Thus, grain boundary sliding can proceed as a sequence of a highly localised shear transformations γ_i, which constitutes iso-configurational flow kinetics based on transition state theory [8,39]. The stresses involved at this stage are of short-range. This process can go on till it is blocked by steric hindrance, e.g., a triple junction, a large precipitate.

(c) As the basic sliding unit is embedded inside a solid matrix, it will also experience a momentary dilation as it moves over a saddle point while going from a stable to the next, nearby stable/ metastable equilibrium configuration under the action of an external stress. The energy associated with the shear and volumetric distortions of the oblate spheroid resulting from unit sliding constitutes the activation energy for the rate controlling GBS process.

(d) As the basic sliding unit embedded in a solid matrix goes from one stable/ metastable configuration to a new state *C*''(=*C*=*C*'), the individual shear component that will remain will depend on the progress of shear in the neighborhood of the basic sliding unit. It is only after the surroundings have been sheared by the same amount that the induced shear will be relaxed completely. This implies that GBS gives rise to an internal stress, whose magnitude will change with the deformation status of the neighborhood and the extent of GBS, i.e., there would be an internal stress distribution resulting from GBS and how to compute this has been explained in [8].

Based on bubble raft experiments and molecular dynamics simulations (for a summary, see [8,15]), for preliminary calculations the average shear strain associated with a unit sliding event (Fig. 2a) is taken as ~ 0.10. (The real value will depend on the free volume present in the basic sliding unit and the interatomic forces between the atoms that constitute the boundary, although the values will hover around 0.1. How it is computed is described below.) When this atomistic-level sliding process reaches the end of a boundary, an externally measurable sliding displacement will result, but at that point steric hindrance in the form of a triple junction will also be present. That will prevent this kind of boundary sliding from proceeding further.

Mesoscopic Boundary Sliding: For substantial elongation, the GBS process has to develop to a mesoscopic scale by the alignment of two or more grain boundaries to form a plane interface (the so called "cooperative boundary sliding", in the words popularized by O. A. Kaibyshev and his colleagues), which by further interconnection with similar plane interfaces present throughout the bulk of the sample leads to long range sliding and superplasticity. For mathematical development, Fig. 2 illustrates some of the ideas explained above through idealized diagrams, assuming the grain size to be of constant value (in real materials there is a grain size distribution and therefore, the constant grain size assumed here would correspond to the mean grain size for a given material state). Fig. 2a is a sketch of the basic sliding unit that contains free volume. The grain shape is taken to be rhombic dodecahedral

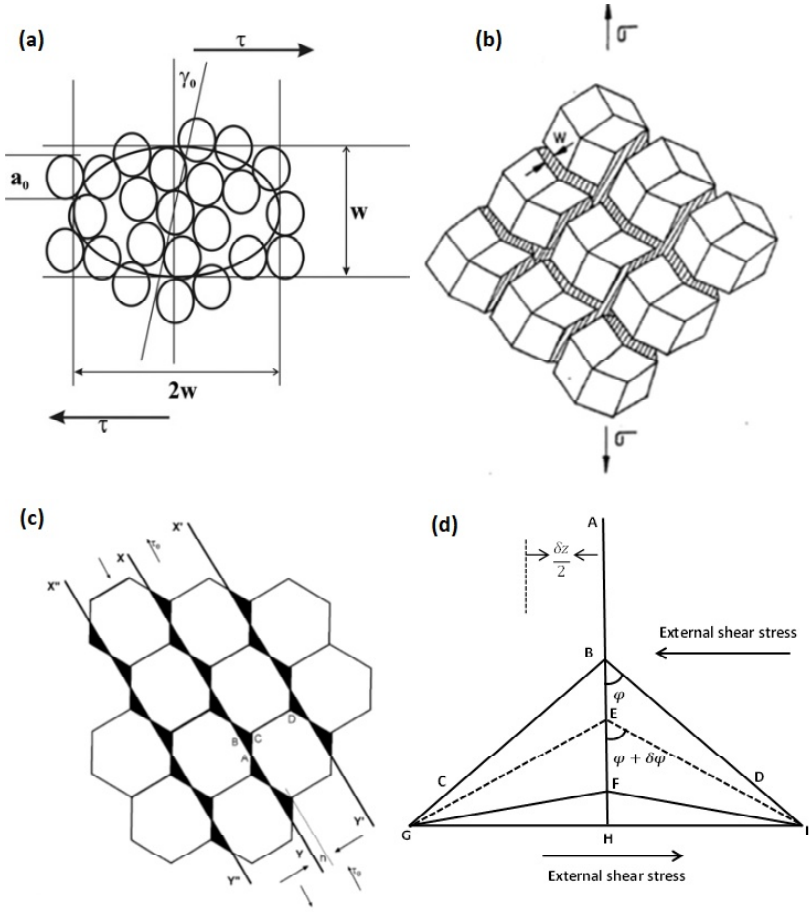

Fig. 2. (a) Basic boundary sliding unit containing free volume. (b) Assuming a rhombic dodecahedral grain shape (closest to the shape of real crystals, see our works [8,21]) the grain boundary regions within which the rate-controlling process is confined are shown shaded. (c) Plane interfaces (the ones like *XY*, *X'Y'*, *X''Y''* etc.) formed by mesoscopic boundary sliding when the atoms located in the shaded regions are moved by the external stress in such a way to extend the boundaries normal to the shear direction to reach the sliding boundary and form a plane interface, (d) an illustration, based on Herring's theory for equilibrium at a triple junction, which illustrates the extension downward of the boundary perpendicular to the external stress axis (AB to AH) to decrease the overall free energy of the system. In the process a plane interface gets formed (adapted from [9,11]).

(Fig. 2b), as it is considered to be the closest to that of real crystals [21]. Evidently, a plane interface will form if the "hills and valleys" present in the shaded portions in Fig. 2c are flattened by a suitable accommodation process. Padmanabhan and Schlipf [8] have derived by an energy balance between the work done by the external stress and the work to be done for flattening the "hills and valleys" shown in the shaded portions of Fig. 2c an expression for the long range threshold stress, τ_0, needed for the formation of the plane interface/commencement of mesoscopic boundary sliding. They and [9] have also pointed out that plane interface formation is in conformity with G I Taylor's principle of maximum work and the generally accepted concept of minimization of the total free energy of a system as a reaction goes forward.

The physical mechanism as to how a triple junction, e.g. ABGI in Fig. 2d, is transformed into a plane interface GHI by AB extending up to ABH was proposed [8] by modifying an idea expressed earlier by Perevezentsev et al. [40]. Briefly, due to boundary sliding events stress concentration develops at the leading end of the sliding boundary. (As the displacement along the boundary due to a single boundary sliding event is only a fraction of the interatomic distance, several events would be necessary to have a total boundary displacement comparable to interatomic spacing.) From that leading end, a dislocation will get emitted into the adjacent grain during a thermal event or in a barrier-free manner, which will relieve the stress concentration built up by boundary sliding, provided two conditions are satisfied: (a) the stress concentration build up reaches

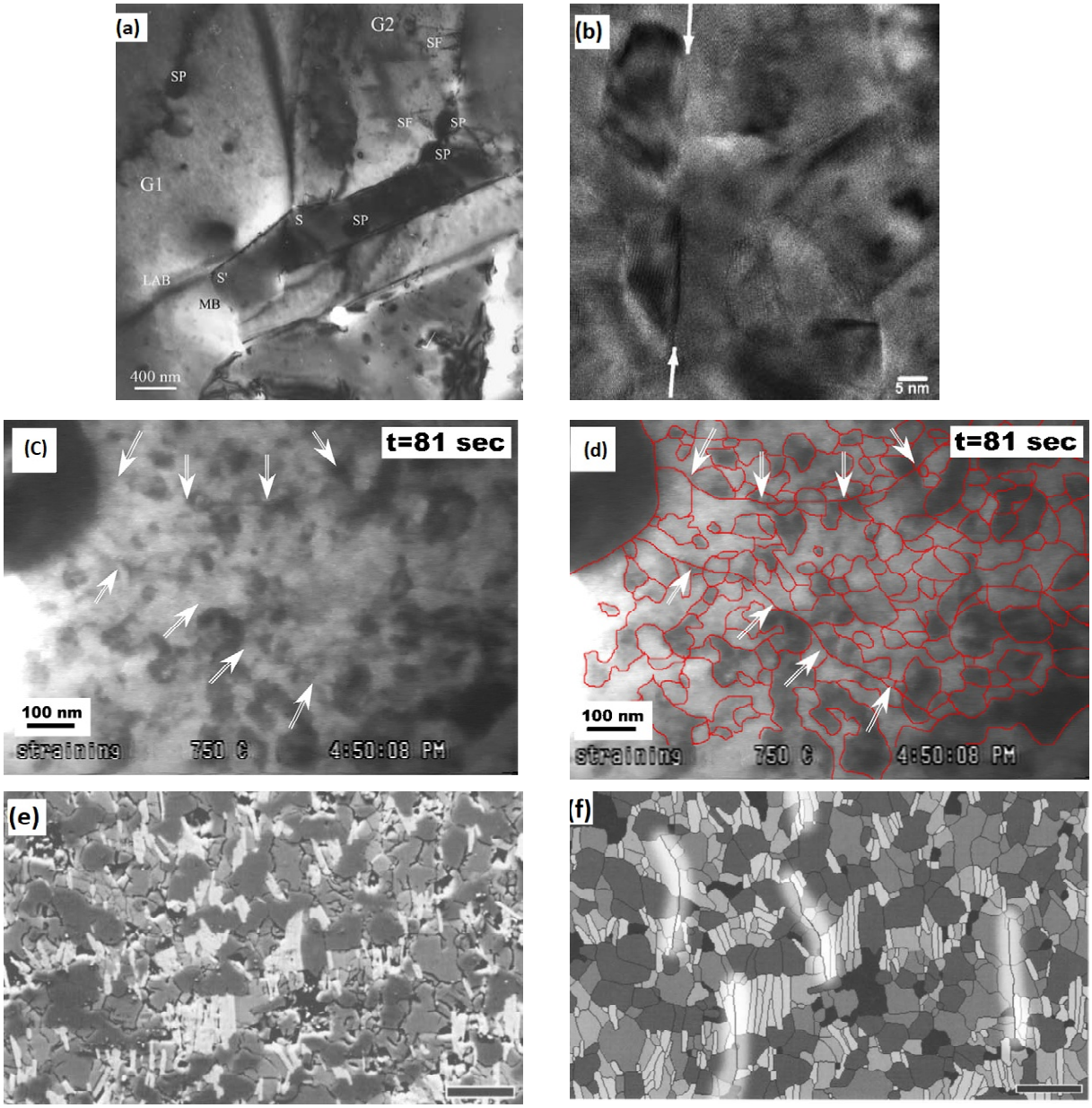

Fig. 3. (a) Electron micrograph showing plane interface formation in a micron-grained Cu-based superplastic alloy, adapted from Gouthama & Padmanabhan, 2003 [43]. (b) High resolution TEM micrograph of nanocrystalline Pd after rolling that shows plane interface formation extending over several grain boundaries (arrowed), adapted from Markmann et al., 2003 [44]. (c) TEM images after 81 s of deformation, taken just after the commencement of mesoscopic boundary sliding. Material tested: Nanocrystalline Ni_3Al. Note "stringers" formed in (c), as highlighted in (d), adapted from Mara et al., 2007 [45]. (e) High magnification Back Scattered Electron (BSE) micrograph of a polished and etched ultra-mylonite showing evidence for plane interface formation. Scale bar: 30 μm. (f) Line drawing after (e) showing the continuous alignment of grain and interphase boundaries across several grain diameters (mesoscopic boundary sliding); several of them are highlighted. Scale bar: 30 μm (adapted from Fliervoet et al., 1997 [46]; proof through a TEM study is yet to be provided).

the value needed to trigger a dislocation into the adjacent grain (a stress/ force constraint), and (b) the "misfit" accumulated as a result of continued GBS at the location from where the dislocation gets emitted equals the Burgers vector appropriate for dislocation motion in the concerned slip system of the adjacent grain (a geometric constraint). Such an emitted dislocation will traverse the (adjacent) grain and get absorbed at an opposite boundary. Evidence for such a process being present during superplastic deformation has been reported experimentally in both microcrystalline and nanocrystalline

materials and in addition by MD simulation of deformation of grain boundaries in nanocrystalline materials.

In fact, it has been observed that such a mechanism persists at least down to 8 nm [11,41,42]. Needless to say, grain boundary diffusion could also be present simultaneously as an accommodation process. But several studies have shown that under conditions of superplastic deformation, rate of diffusion in the GB regions is rather slow [1,2]. However, below a grain size (e.g., < 8 nm) and stresses less than a critical value below which dislocation emission will not be possible (due to the stress constraint stated above [40] not being satisfied), there is a possibility that plane interface formation takes place only by diffusion. In contrast, the diffusion distances would be too long in two- or multi-phase materials. Therefore, plane interface formation in those types of materials can only take place by the dislocation emission mechanism described above. Some experimental results that support the concept of plane interface formation are presented as Figs. 3a – 3f.

Thus, an effective stress, $(\tau-\tau_0)$, where τ is the externally applied shear stress and τ_0 is the threshold shear stress needed for the commencement of mesoscopic boundary sliding, is available to drive superplastic deformation. Calculations reveal that the long-range threshold stress, τ_0, is given by [8-10]

$$\tau_0 = \left(2G\gamma_B\right)^{0.5}\left[\frac{0.6204}{N^{0.5}d}\right]^a. \tag{3}$$

Here γ_B is the specific grain boundary energy (assumed to be isotropic), which obeys the constraint $0 < \gamma_B < 1.5$ Jm^{-2} and N is the number of boundaries that align to form a plane interface that obeys the constraint $0 < N < 20$ (arrived at based on the limited number of experimental observations of plane interfaces observed in different systems, e.g. Fig. 3). d is the mean grain size (and the grain shape, as stated earlier, has been assumed to be rhombic dodecahedral). If the grain size and shape are constant, "a" will equal 0.50 [8]. When the grain shape is irregular and there is a grain size distribution, "a" obeys the condition $0 < a < 0.50$ [10].

Following Eshelby, the activation energy for the rate controlling process is computed as [8,37]

$$\Delta F_0 = \frac{1}{2}\left(\beta_1\gamma_0^2 + \beta_2\varepsilon_0^2\right)GV_0, \tag{4}$$

where G is the shear modulus. The volume of the basic sliding unit (oblate spheroid), $V_0 = (2/3)\pi/W^3$, where W is the average grain boundary width. For an oblate spheroid shape $\beta_1 = 0.944(1.590-p)/(1-p))$, $\beta_2 = 4(1+p)/9(1-p)$ with p the Poisson ratio [37]. The von Mises yield behavior is assumed for the calculations presented here, but it has also been demonstrated that even when a hydrostatic-stress-system-dependent yield criterion is used, e.g., Mohr-Coulomb, no significant changes in the results are found [13, 14]. As a result, the relationships $\sigma = 3^{0.5}\tau$, $\sigma_0 = 3^{0.5}\tau_0$, and $\dot{\varepsilon} = (\dot{\gamma}/3^{0.5})$ are used in the analysis. Mathematical development of the ideas [8-12] has led to the rate equation

$$\dot{\gamma} = 0 \text{ when } \tau < \tau_0, \tag{5a}$$

$$\dot{\gamma} = \frac{2W\gamma_0\nu}{d}\sinh\left(\frac{\left(\tau-\tau_0\right)\gamma_0V_0}{2kT}\right)\times \exp\left(-\frac{\Delta F_0}{kT}\right) \text{ if } \tau > \tau_0. \tag{5b}$$

In the above equation $\dot{\gamma}$ is the shear strain rate of deformation, γ_0 is the mean shear strain associated with an atomic scale sliding event at a basic sliding unit (taken to be equal to 0.10 as a starting value in the numerical computations and later refined- see below). W, the average grain boundary width is equal to ~$2.5a_0$ where a_0 is the diameter of the concerned atom species [38]. ν the thermal vibration frequency equals (kT/h) or 10^{13} s^{-1}, k is the Boltzmann constant, h is Planck's constant and T is the temperature of deformation on the absolute scale.

3. ALGORITHM AND COMPUTATIONAL PROCEDURE

It is seen from the transcendental Eq. (5b) that there are no adjustable/ ill-defined constants in the analysis and every constant is either already known from literature or can be calculated using the equations derived here. The algorithm developed for validating the mesoscopic GBS-controlled flow model for optimal structural superplasticity [12] uses the following input data taken from the experimental results concerning any given system: stress - strain rate pairs taken from the optimal flow region, where the stain rate sensitivity index, m, increases with increasing strain rate; the atomic diameter, a_0, of the main species when its volume fraction in the alloy is greater than 0.9 or an average value for all the major elements present, obtained using the rule of mixtures; shear modulus, G and the coefficient that reveals its variation with temperature, C_d, taken from the well-known compilation of Frost and Ashby [47].

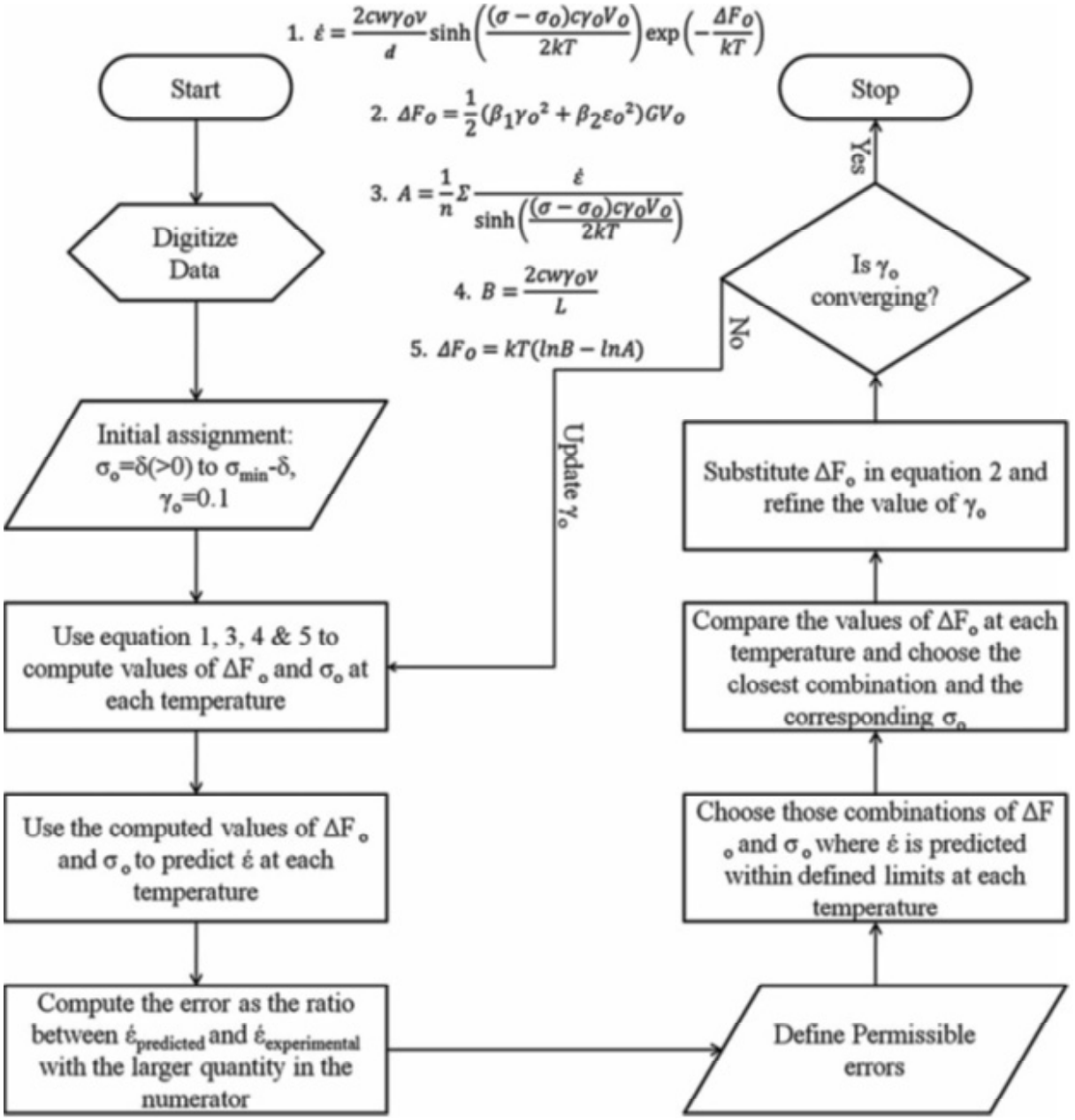

Fig. 4. Flow chart describing the algorithm used for computing the free energy of activation, ΔF_0, the unit shear strain γ_0, the threshold stress for the onset of mesoscopic boundary sliding, σ_0 and for predicting the strain rate under the given experimental conditions, $\dot{\varepsilon}$ (see our work [12]).

The other required properties for the analysis, viz., melting temperature, T_m and Poisson's ratio, p were taken from literature. When p is unknown, its value is set as 0.33. The flow chart describing the algorithm used for computing the free energy of activation ΔF_0, γ_0 the value of the unit shear strain, σ_0 the threshold stress required for the onset of mesoscopic boundary sliding and the prediction of strain rate, $\dot{\varepsilon}$, is presented in Fig. 4.

For a given temperature and grain size a set N_1 pairs of log (stress) - log (strain rate) values (as large as possible, taken within the optimal region up to the point of inflection in the isothermal log stress- log strain rate plot) is chosen. The algorithm consists of the following major steps. To start with, as stated above, the value of unit shear strain is taken as equal to 0.10 and the two unknowns σ_0 and ΔF_0 are computed at each temperature as follows: (a) By definition, the upper limit for the threshold stress is smaller than the smallest experimentally measured stress at which positive flow has been observed. (b) Using Eq. (5b), the activation energy

ΔF_0 is calculated using the method of least squares for each possible τ_0 value between 0 and the upper limit selected in (a). (c) Then, using all the ΔF_0, σ_0 values obtained, the strain rate was re-predicted for each of the external stress value used in the analysis. The ΔF_0, σ_0 combination for which the predicted values were the closest to the experimentally observed values of the strain rate was chosen as the best fit combination. (d) The procedure was repeated with smaller iteration step sizes around the best threshold stress value from the previous step until the required precision is obtained, with a proviso that ΔF_0 is practically independent of temperature, as required by Arrhenius kinetics.

As the value of γ_0 used in the calculations was a rough estimate obtained by MD simulations and bubble raft experiments, its accurate value for each system was calculated using an iterative procedure [12] involving Eq. (4) and the value of ΔF_0 obtained in step (d) above. The value of free energy of activation computed using the numerical procedure described in the previous paragraph was matched with the one obtained by Eq. (4) and the value of the unit shear strain was adjusted iteratively as shown in the flow chart until a value of γ_0 that leads to the closest (desired) proximity between the two ΔF_0 values (predicted by Eq. (4) and the one calculated from Eq. (5b) by the numerical analysis) is obtained.

Thus, at each temperature the transcendental Eq. (5b) was solved numerically using the algorithm and the strain rates were predicted for different σ_0 and ΔF_0 combinations at different stress levels. The best ΔF_0 value which satisfies the condition of temperature independence and the corresponding σ_0 value which allows the closest match between the experimentally measured and the predicted strain rates was selected as the "best fit" values for a given material. The standard deviation (SD), average error (AE) and correlation coefficient (CC) were the statistical measures used to determine the accuracy of predictions. Evidently, the model and the analytical procedure do not involve any adjustable constants and the unknowns of the rate equation (Eq. (5b)) can be obtained directly using the flow chart and the algorithm presented in Fig. 4.

4. RECENT DEVELOPMENTS

It is clear from the analysis presented up to here that steady state optimal structural superplasticity is a two constant (ΔF_0, σ_0) problem, whose values are obtained from experimental results. More recently, it has been possible to propose that the phenomenon can be described in terms of four "universal" constants, which are independent of the material system. For knowing the shear modulus of any material at any given temperature the equations proposed by Frost and Ashby [47] are used.

The method of obtaining the refined value of γ_0 for any material from the experimental results was explained in the previous section. From Eq. (3), it is seen that σ_0 ($=3^{0.5}.\tau_0$)3 is a function of three unknowns, viz., γ_B ($0< \gamma_B <1.5$ J.m^{-2}; experimentally determined limits), N ($1 < N < 20$; experimentally determined limits) and a ($0 < a < 0.5$; experimentally determined limits). It is also clear that σ_0 is a function of temperature and grain size, but is independent of stress/ strain rate. Thus by using more than 3 (this number should be as large as possible for good accuracy) σ_0 values and the method of least squares, the "the best fit" values of γ_B, N and "a" for every material of a given grain size undergoing deformation at a specified temperature are obtained. Using this approach, the values of the four constants (of γ_0, γ_B, N, and "a") for 25 materials systems, drawn from different classes like metals and alloys, ceramics, composites, geological materials, ice etc., for different grain sizes and temperatures were determined. Averages of the different values of these four constants were taken to obtain a set of four material-independent constant values. With the help of these four "universal" constants and the Frost-Ashby equations [47] for knowing the value of the shear modulus of any material at any given temperature, it is possible to predict the strain rate for any combination of stress, grain size and temperature corresponding to any material, including those that were not used to obtain the four constants. As these are unpublished results, they will be published separately elsewhere (although these results will be displayed during the lecture at ICSAM 2018). A short paper based on this approach is also being presented at ICSAM 2018 [17].

In recent years, O. A. Kaibyshev and his colleagues, like the present authors since 1977, have emphasized that GBS controls the rate of optimal superplastic deformation. More recently, Valiev and Nazarov [48] have informed the first author that they no longer insist on GBS propagating by the glide of grain boundary dislocations. They now talk in terms of the propagation of "mesoscopic defects" in a mesoscopic sense (to avoid a conflict with Gleiter's structural unit model). To this we have no objection because as pointed out in [11] the deformation of an oblate spheroid would leave a closed dislocation loop in a "Volterra sense" (as opposed to a crystallographic sense), which from outside the loop will have zero Burgers vector (and qualify as an "ex-

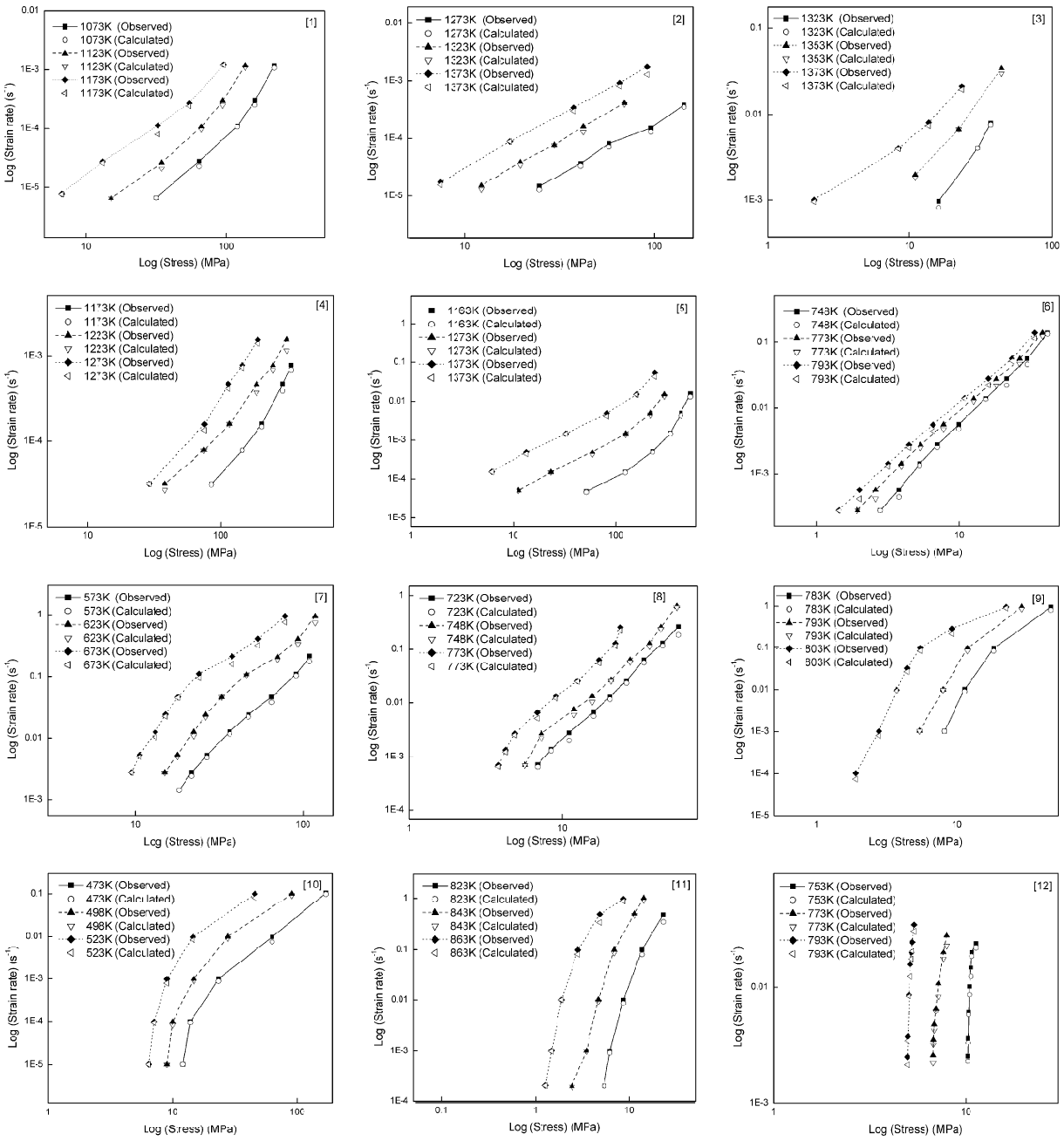

Fig. 5. Strain rate as a function of flow stress at different temperatures for the alloys numbered 1-12 in the Appendix. Experimental data are connected by curves. Calculated values were obtained using Eq. (5b).

trinsic dislocation in a Volterra sense"), while at any point on the circular loop it will have a Burgers vector, which would only be a very small fraction of the inter-atomic distance. An "MD simulation experiment" has been planned to verify if the displacement due to unit boundary sliding predicted in [11] is correct. Further details in this regard also will be published elsewhere.

5. EXPERIMENTAL VALIDATION

Stress-strain rate data pertaining to 12 systems [49-60] were used for the validation of the computational method described in this paper. It is demonstrated below that the mesoscopic grain boundary sliding-controlled flow model predicts the strain rates very accurately for the classes of materials chosen here of grain sizes as mentioned in the figures and tested under different temperature and stress conditions. The tolerance is defined as the ratio of $\dot{\varepsilon}_{experimental}$ to $\dot{\varepsilon}_{predicted}$ with the larger of the two values appearing in the numerator. If this value is less than 10 the fit is considered to be good (an order of magnitude accuracy). Excellent predictions were observed for all the systems analyzed here (Fig. 5), with the

minimum and maximum tolerances being ~1.12 and ~1.98 respectively (a very close agreement between the experimental results and the predictions indeed). In the Appendix, results related to some intermetallics and materials that exhibit high strain rate superplasticity, as analyzed earlier [13,14] and also now using the current program, are presented. Evidently, the present predictions are better and the new algorithm is statistically more robust.

6. CONCLUDING REMARKS

A physical model in which grain/ interphase boundary sliding that develops to a mesoscopic scale (of the order of a grain diameter or more) controls the rate of superplastic flow is proposed. While this model has been shown to apply to all classes of superplastic materials (unpublished work), in this paper it is validated using the experimental data pertaining to five different intermetallics and seven materials that display high strain rate superplasticity. The grain sizes range from 0.65 μm to 24 μm and the strain rates vary from ~ 10^{-6} s^{-1} to 10 s^{-1}. The temperature spread also is extensive. Using the rigorous numerical procedure developed, excellent predictions of the strain rate have been achieved using two physically meaningful constants, viz., the activation energy for the rate controlling process, ΔF_0 and the threshold stress needed for the onset of mesoscopic boundary sliding, σ_0 whose magnitudes are obtained accurately from the experimental data. In addition, the unit shear strain associated with unit boundary sliding event follows in all cases the expected trend of increasing magnitude with increasing temperature (Appendix). The long-range threshold stress for the onset of mesoscopic boundary sliding also follows in all cases the expected trend of decreasing magnitude with increasing temperature (Appendix). The free energy of activation for similar materials, calculated from the experimental data reported by different investigators turn out to be similar/comparable (Appendix), as should be the case in a sound analysis. It is also mentioned that the phenomenon of steady state optimal structural superplasticity in all classes of materials can be reduced to four "universal" constants and the Frost-Ashby equations can be used to predict the shear modulus of any material at any temperature. Detailed results in this regard will be published elsewhere. In recent times our viewpoint on this phenomenon and the approach adopted by the Russian School headed by O.A. Kaibyshev, R.Z. Valiev, and others have been reconciled. Some crucial MD simulation experiments have been planned for further confirmation of the similarity of the views of the two schools. The point mentioned last (unpublished work) will also be discussed in detail elsewhere.

ACKNOWLEDGEMENT

Academician (Prof.) O.A. Kaibyshev was a true friend of K.A. Padmanabhan (KAP), whom the latter will miss till the end of his life. When Academician Kaibyshev was the President of the Bashkirian Academy of Sciences, in September 1991 KAP was elected an Honorary Academician of the above academy. This was two years prior to KAP's election as a Fellow of the Indian Academy of Sciences and the Indian National Academy of Engineering, three years before his receiving the "Forschungspreis" of the Alexander von Humboldt Foundation, Germany and seven years before he received an ScD from University of Cambridge, UK. During the days Oskar was at the height of his powers, India was very close to Russia. Today, Russia is equidistant between China and India and India is a strategic partner of the USA. Nations change, politics change, but true friendship among people is everlasting. With this solemn recognition, this paper is dedicated to the sacred memory of Academician (Prof.) Oskar Akramavich Kaibyshev.

APPENDIX: SUMMARY OF THE RESULTS OF THE ANALYSIS*.

Serial and Ref. No	System	Temp (K)	Grain size (μm)	ΔF_0 (kJmol^{-1})	γ_0	σ_0 (MPa)	Tolerance
1 [49]	TiAl	1073	0.8	262	0.1131	39.62	1.77
		1123		271	0.1179	17.25	1.21
		1173		277	0.1222	9.49	1.17
2 [50]	Ti-43Al	1273	5	282	0.1305	20.83	1.13
		1323		286	0.1353	9.79	1.78
		1373		292	0.1413	5.28	1.71

3 [51]	Ni3Si	1323	15	226	0.1482	12.35	1.85
		1353		221	0.1499	7.57	1.41
		1373		224	0.1532	0.82	1.75
4 [52]	Co3Ti	1173	24	221	0.1288	5.73	1.98
		1223		225	0.1340	2.63	1.87
		1273		229	0.1397	2.01	1.93
5 [53]	Ti-Al	1163	0.9	280	0.1223	17.20	1.06
		1273		285	0.1312	6.75	1.32
		1373		290	0.1409	3.72	1.12
6 [54]	Al-5Mg	748	24	129	0.0719	23.50	1.23
		773		132	0.0734	15.58	1.70
		793		134	0.0745	11.95	1.51
7 [55]	Al-5.76Mg	573	1.2	107	0.0616	12.94	1.46
		623		104	0.0620	12.93	1.74
		673		106	0.0633	9.95	1.51
8 [56]	Al-5.76Mg	723	3	123	0.0694	4.21	1.62
		748		125	0.0707	3.37	1.74
		773		127	0.0721	2.07	1.55
9 [57]	Al-17Si	783	1.4	134	0.1049	7.54	1.36
		793		135	0.1050	4.91	1.31
		803		134	0.1077	1.71	1.58
10 [58]	Mg-6Zn	473	0.65	95	0.0998	11.54	1.46
	-0.8Zr	498		98	0.1017	8.65	1.32
		523		99	0.1033	6.27	1.28
11 [59]	6061/	823	2.6	128	0.1219	6.08	1.61
	20%SiC_w	843		129	0.1221	1.78	1.59
		863		124	0.1235	0.75	1.33
12 [60]	7075/	753	1.75	118	0.1129	9.56	1.63
	20%SiC_w	773		118	0.1139	6.46	1.42
		793		116	0.1141	4.46	1.34

REFERENCES

[1] K.A. Padmanabhan and G.J. Davies, *Superplasticity* (Springer- Verlag, Heidelberg, Berlin, 1980).

[2] O.A. Kaibyshev, *Superplasticity in alloys, intermetallides and ceramics* (Springer-Verlag, Heidelberg, Berlin, 1992).

[3] T.G. Nieh, J. Wadsworth and O.D. Sherby, *Superplasticity in metals and ceramics* (University Press, Cambridge 1997).

[4] A.K. Mukherjee // *Mater. Sci. Eng*. **322** (2002) 1.

[5] C.E. Pearson //*J. Inst. Met.* **54** (1934) 111.

[6] K.A. Padmanabhan, R.A. Vasin and F.U. Enikeev, *Superplastic Flow: Phenomenology and Mechanics* (Springer-Verlag, Heidelberg, 2001).

[7] A.Ball and M.M. Hutchison // *Met. Sci. J.* **3** (1969) 1.

[8] K.A. Padmanabhan and J. Schlipf // *Materials Science and Technology* **12** (1996) 3991.

[9] K.A. Padmanabhan and H. Gleiter // *Mater. Sci. and Eng.: A* **381** (2004) 28.

[10] T.A. Venkatesh, S.S. Bhattacharya, K.A. Padmanabhan and J. Schlipf // *Materials Science and Technology* **12** (1996) 635.

[11] K.A. Padmanabhan and H. Gleiter // *Current Opinion in Solid State and Materials Science* **16** (2012) 243.

[12] S. Sripathi and K.A. Padmanabhan // *J. Mater. Sci.* **49** (2014) 199

[13] K.A. Padmanabhan and M.R. Basariya // *Int J Mater Res (Former Z Metallk.)* **100** (2009)1543.

[14] K.A.Padmanabhan and M.R. Basariya // *Mater. Sci. and Eng.: A* **527** (2009) 225.

[15] K.A. Padmanabhan // *J Mater Sci* **44** (2009) 2226.

[16] J. Buenz, K.A. Padmanabhan and G. Wilde // *Intermetallics* **60** (2015) 50.

[17] M. R. Basariya and K. A. Padmanabhan // *Materials Science Forum* (in press).

[18] K.A. Padmanabhan, G.P. Dinda, H. Hahn and H. Gleiter // *Mater. Sci. Eng. A* **452–453** (2007) 462.
[19] K.A. Padmanabhan, Sripathi Sriharsha, H. Hahn and H. Gleiter // *Materials Letters* **133** (2014) 151.
[20] M. R. Basaria, N. K. Mukhopadhyay, S. Sripathi and K.A. Padmanabhan // *Journal of Alloys and Compounds* **673** (2016) 199.
[21] H. Hahn and K.A. Padmanabhan // *Philos Mag Part B* **76** (1997) 559.
[22] U. Betz, K.A. Padmanabhan and H. Hahn // *J Mater. Sci*. **36** (2001) 5811.
[23] S. Sripathi and K.A. Padmanabhan // *Mater. Sci. Forum* **735** (2012) 246.
[24] P. M. Hazzledine and D. E. Newbury, In: *Proc. 3rd Int. Conf. on Strength of Metals, Inst. Metals* vol. **1** (1973), p. 292.
[25] A.K. Mukherjee, *Superplasticity in Metals, Ceramics and Intermetallics,* In: *Materials Science and Technology*, Vol. **6,** ed. by R.W. Chan, P. Haasen and E.J. Kramer (VCH Publishers, Weinheim 1993), p. 302.
[26] A.K. Mukherjee, J.E. Bird and J.E. Dorn // *Trans. ASM* **62** (1969) 155.
[27] K.A. Padmanabhan, J. Leuthold, G. Wilde and S.S. Bhattacharya // *Mechanics of Materials* **91** (2015) 177.
[28] T. G. Langdon // *Acta Metall. et Mater*. **42** (1994) 2437.
[29] I.A. Ovid'ko // *Reviews on Advanced Materials Science* **10** (2005) 89.
[30] K. A. Padmanabhan and H. Gleiter // *Beilstein J. Nanotechnol*. **5** (2014) 1603.
[31] A. P. Sutton and V. Vitek // *Philos. Trans. Roy. Soc. (London) A* **309** (1983) 55.
[32] A. P. Sutton and V. Vitek // *Philos. Trans. Roy. Soc. (London) A* **309** (1983) 37.
[33] A. P. Sutton and V. Vitek // P*hilos. Trans. Roy. Soc. (London) A* **309** (1983) 1.
[34] A. P. Sutton, R.W. Baluffi and V. Vitek // *Scr. Metall.* **15** (1981) 989.
[35] A. P. Sutton // *Philos. Mag. A* **46** (1982) 171.
[36] D. Schwartz, V. Vitek and A.P. Sutton // *Philos. Mag. A* **51** (1985) 499.
[37] J.D. Eshelby //*Proceedings of the Royal Society of London. Series A, Mathematical and Physical Sciences* **241** (1957) 376.
[38] P. Haasen, *Physical Metallurgy* (Cambridge University Press, UK, 1978).
[39] A.S. Argon // *ActaMetall.* **27** (1979) 47.
[40] V.N. Perevezentsev, V.V. Rybin and V.N. Chuvil'deev // *Acta Metall. Mater.* **40** (1992) 895.
[41] H Gleiter, *personal communication.*
[42] M. Grewer and R. Birringer // *Physical review, B* **89** (2014) 184108.
[43] Gouthama and K.A. Padmanabhan // *Scripta Materialia* **49** (2003) 761.
[44] J. Markmann, P. Bunzel, H. Rosner, K.W. Liu, K.A. Padmanabhan, R. Birringer, H. Gleiter and J. Weissmuller // *Scripta Materialia* **49** (2003) 637.
[45] N.A. Mara, A.V. Sergueeva, T.D Mara, S.X. McFadden and A.K. Mukherjee // *Materials Science and Engineering A* **463** (2007) 238.
[46] T.F. Fliervoet, S.H. White and M.R Drury // *Journal of Structural Geology* **19** (1997) 1495.
[47] H.J. Frost and M.F. Ashby, *Deformation-mechanism maps: the plasticity and creep of metals and ceramics* (Pergamon Press, Oxford, UK, 1982).
[48] R.Z. Valiev and A.A. Nazarov, *personal communication*.
[49] J. Sun, Y.H. He and J.S. Wu // *Mater.Sci. Eng. A* **329-331** (2002) 885.
[50] T.G. Nieh and J. Wadsworth // *Mater. Sci. Eng.A* **239-240** (1997) 88.
[51] T.G. Nieh and W.C. Oliver // *Scr. Metall.* **23** (1989) 851.
[52] W.Y. Kim, S. Hanada and T. Takasugi // *Acta Mater*. **46** (1998) 3593.
[53] G. Wegmann, R. Gerling, F.P. Schimansky, H. Clemens and A. Bartels // *Intermetallics* **10** (2002)511.
[54] R. Kaibyshev, E. Avtokratova, A. Apollonov and R. Davies // *Scr. Mater*. **54** (2006) 2119.
[55] F. Musin, R. Kaibyshev, Y. Motohashi and G. Itoh // *Scr. Mater.* **50** (2004) 511.
[56] T.G. Nieh, L.M. Hsiung, J. Wadsworth and R. Kaibyshev // *Acta Mater.* **46** (1998) 2789.
[57] S. Fujino, N. Kuroishi, M. Yoshino, T. Mukai, Y. Okanda and K. Higashi // *Scr. Mater.* **37** (1997) 673.
[58] H. Watanabe, T. Mukai, K. Ishikawa, M. Mabuchi and K. Higashi // *Mater. Sci. Eng. A* **307** (2001) 119.
[59] T.D. Wang and J.C. Huang // *Mater. Trans*. **42** (2001) 1781.
[60] Y. Nishida, I. Sigematsu, H. Arima, J.-C. Kim and T. Ando // *J. Mater. Sci. Lett.* **21** (2002) 465.